Supplement of Atmos. Chem. Phys., 26, 10379–10398, 2026
https://doi.org/10.5194/acp-26-10379-2026-supplement

Atmospheric Chemistry and Physics
Open Access
EGU

Supplement of

Spatiotemporal optimization of NO_x and VOC emissions using a hybrid inversion framework and implications for ozone sensitivity-regime diagnosis

Jeonghyeok Moon et al.

Correspondence to: Wonbae Jeon (wbjeon@pusan.ac.kr)

Table S1: Model configurations of the Weather Research and Forecasting (WRF) simulation.

WRF	Domain 01(D1)	Domain 02(D2)
Horizontal Resolution (Number of grids)	27 km (150 × 135)	9 km (79 × 79)
Vertical layers	35 Layers	
Microphysics option	WSM 3-class simple ice scheme	
Radiation option	RRTM scheme(long-wave) Dudhia scheme(short wave)	
Surface layer option	Revised MM5 Monin-Obukhov scheme (Jimenez)	
Land-surface option	Unified Noah land-surface model	
PBL option	YSU scheme	
Cumulus option	Kain-Fritsch (new Eta) scheme	
Initial data	ERA5 (0.25˚ × 0.25˚)	
Simulation period	2022. 04. 26. 00 UTC – 2022. 05. 16. 00 UTC	

Table S2: Model configurations of the Community Multiscale Air Quality (CMAQ) simulation.

CMAQ	Domain 01(D1)	Domain 02(D2)
Horizontal Resolution (Number of grids)	27 km (137 × 122)	9 km (66 × 66)
Vertical layers	15 Layers	
Anthropogenic emission	EDGAR_HTAPv3	
Biogenic emission	MEGANv2.1	
Chemical mechanism	cb05cl_ae5_aq	
Simulation period	2022. 04. 27. 00 UTC – 2022. 05. 15. 00 UTC	

Table S3: List of VOC species included in this study according to the carbon bond mechanism version 2005 (CB05).

Model species	Definition
ALD2	Acetaldehyde
ALDX	Aldehydes with 3 or more carbons
ETH	Ethene
ETHA	Ethane
FORM	Formaldehyde
IOLE	Internal alkene bond
ISOP	Isoprene
MEOH	Methanol
NVOL	Non-volatile compounds
OLE	Terminal alkene bond
PAR	Carbon-carbon single bond
TERP	Monoterpenes
TOL	Toluene and other monoalkyl aromatics
UNR	Unreactive
XYL	Xylene

Table S4. Statistical metrics used for evaluating model performance and inverse modeling results. Here, n is the total number of compared points, O_i is the observed value or ideal emission value, and M_i is the value of the CMAQ model value.

Descriptions	Metrics	Formula
Mean observation	$\bar{O}$	$\frac{\sum_{i=1}^{n} O_i}{n}$
Mean model	$\bar{M}$	$\frac{\sum_{i=1}^{n} M_i}{n}$
Mean bias error	MBE	$\frac{\sum_{i=1}^{n}(M_i - O_i)}{n}$
Root mean square error	RMSE	$\sqrt{\frac{\sum_{i=1}^{n}(M_i - O_i)^2}{n}}$
Index of agreement	IOA	$1 - \frac{\sum_{i=1}^{n}(M_i - O_i)^2}{\sum_{i=1}^{n}(\lvert M_i - \bar{O}\rvert + \lvert O_i - \bar{O}\rvert)^2}$
Correlation coefficient	r	$\sum_{i=1}^{n}((\frac{O_i - \bar{O}}{\sqrt{\sum_{i=1}^{n}(O_i - \bar{O})^2}}) \times (\frac{M_i - \bar{M}}{\sqrt{\sum_{i=1}^{n}(M_i - \bar{M})^2}}))$
Normalized mean error	NME	$\frac{\sum_{i=1}^{n}\lvert M_i - O_i\rvert}{\sum_{i=1}^{n} O_i} \times 100\ [\%]$

Table S5. Statistical evaluation of 2 m temperature, 2 m relative humidity, and 10 m wind speed from the WRF simulation. Observational data were obtained from ASOS stations.

	OBS	WRF	MBE	RMSE	IOA	r
Temperature [°C]	16.03	14.88	-1.16	2.35	0.94	0.91
Wind speed [m s^{-1}]	1.93	3.19	1.25	1.90	0.68	0.60
Relative humidity [%]	59.74	62.89	3.16	12.95	0.90	0.82

Table S6. Statistical evaluation of NO_2 and O_3 concentrations for the Prior and Hybrid_NOx+VOC experiments at the independent validation sites. The statistics were calculated over the 123 withheld AQMS_VERI sites shown in Fig. S2 and averaged over the entire study period. Observations were obtained from the AQMS network.

Species	Experiment	Obs.	CMAQ	MBE	RMSE	IOA	r
AQMS NO_2 [ppb]	Prior	8.69	9.53	0.84	11.50	0.58	0.44
	Hybrid_NOx+VOC		6.58	-2.11	7.33	0.67	0.48
AQMS O_3 [ppb]	Prior	46.56	43.54	-3.02	16.60	0.71	0.53
	Hybrid_NOx+VOC		47.42	0.86	13.65	0.77	0.64

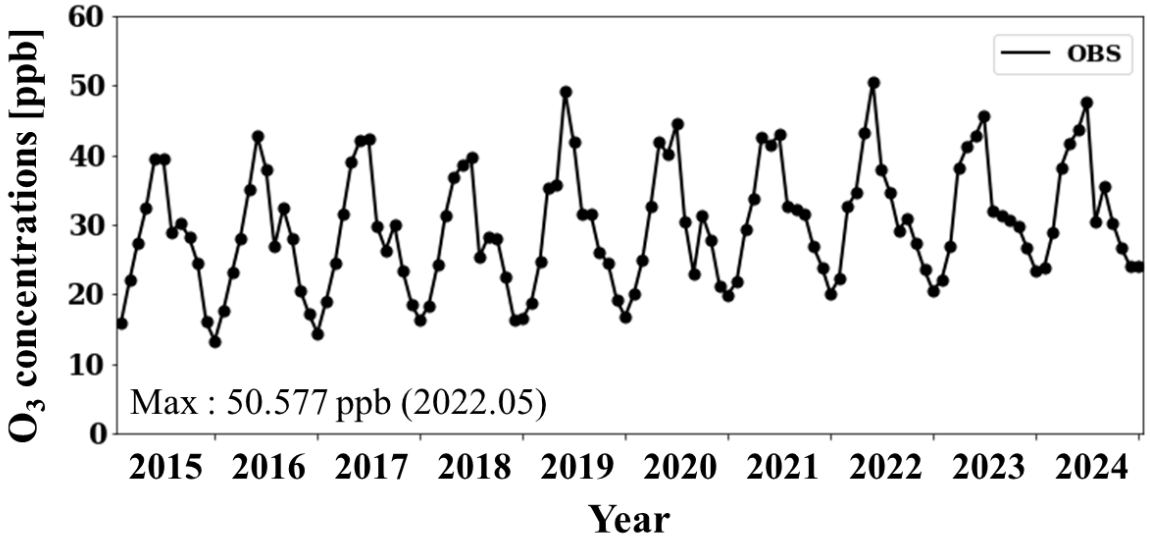

Figure S1: Monthly averaged time series of observed O_3 concentrations over South Korea during the recent decade (2015–2024), based on the AQMS network.

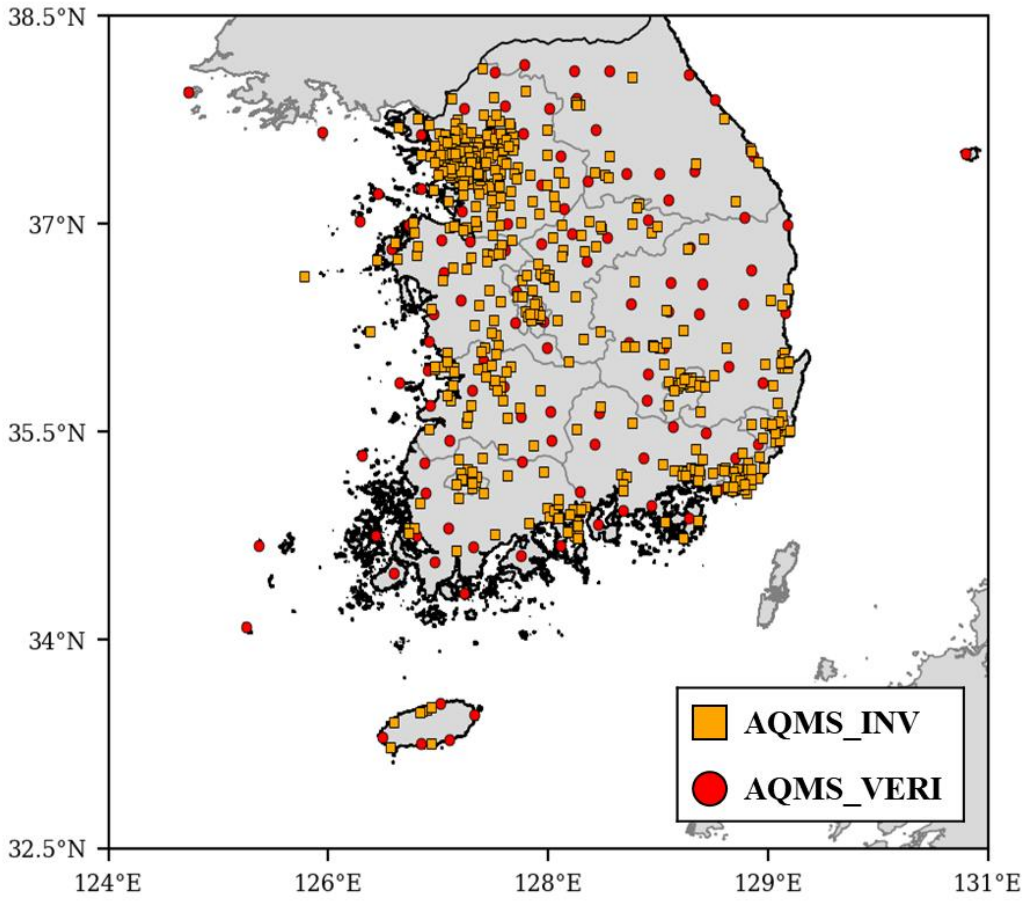

Figure S2: Spatial distribution of AQMS sites used in this study. A total of 619 sites were considered, among which 496 sites (80%) were randomly selected for the inversion (AQMS_INV; orange squares) and the remaining 123 sites (20%) were reserved for independent validation (AQMS_VERI; red circles).

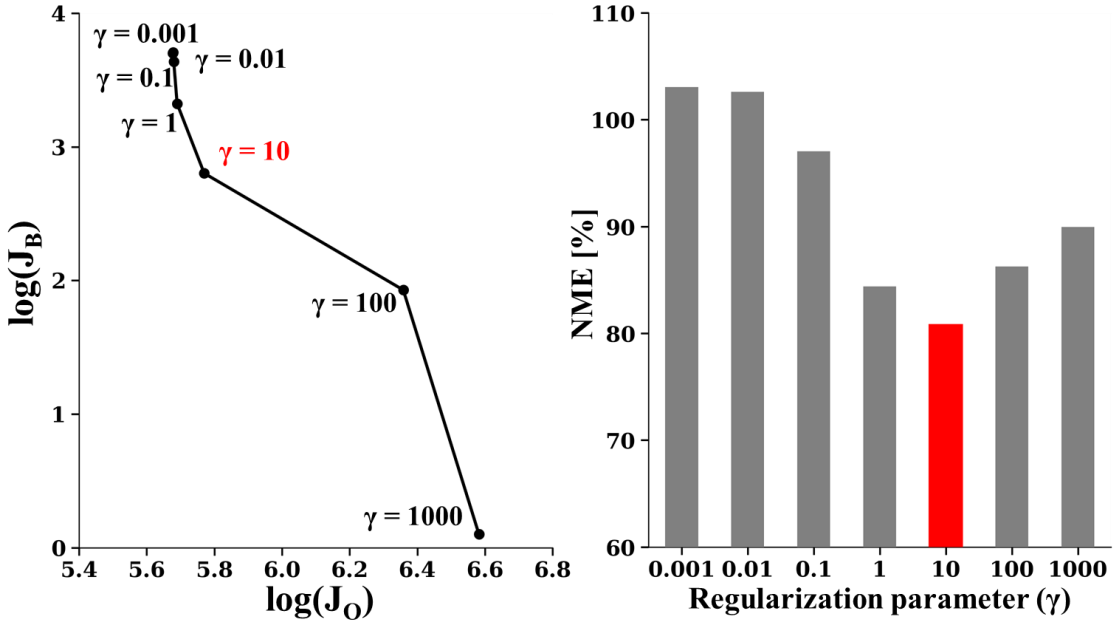

Figure S3: Results of the L-curve test and emission NME [%] used to determine the optimal regularization parameter (γ) for the 4D-Var inverse modeling. J_B represents the background penalty term (the first term on the right-hand side of Eq. (8)) and J_O represents the observation penalty term (the second term on the right-hand side of Eq. (8)). The test was performed for γ values of 0.001, 0.01, 0.1, 1, 10, 100, and 1000, based on the simulation for 1 May 2022. The optimal value was determined to be $\gamma = 10$.

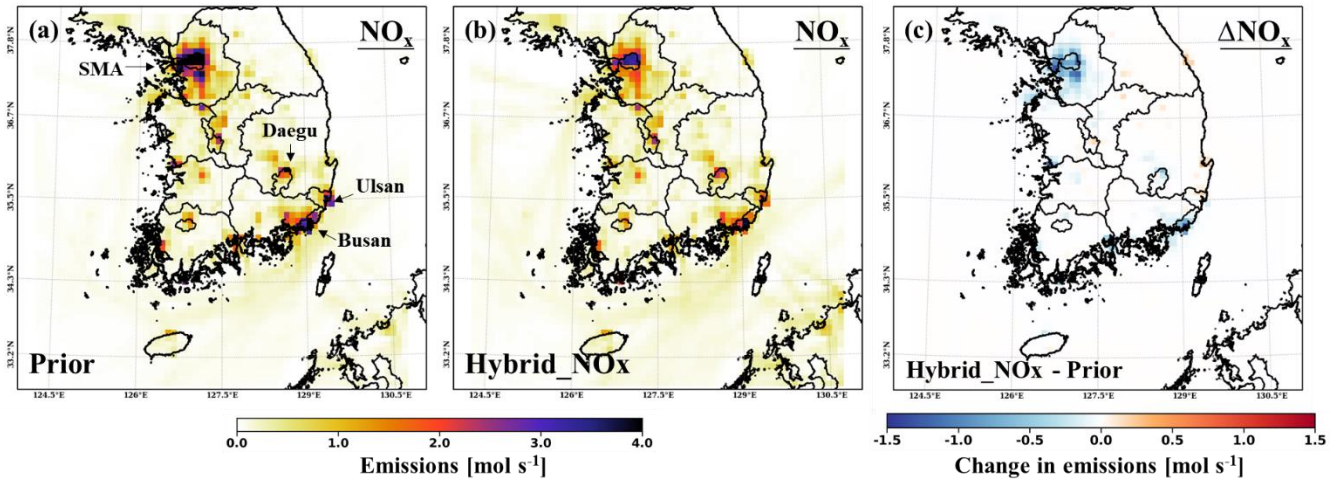

Figure S4: Spatial distributions of (a) the Prior emissions, (b) the Hybrid_NOx emissions, and (c) the corresponding analysis increments (Hybrid_NOx – Prior) for NO_x, averaged over the study period.

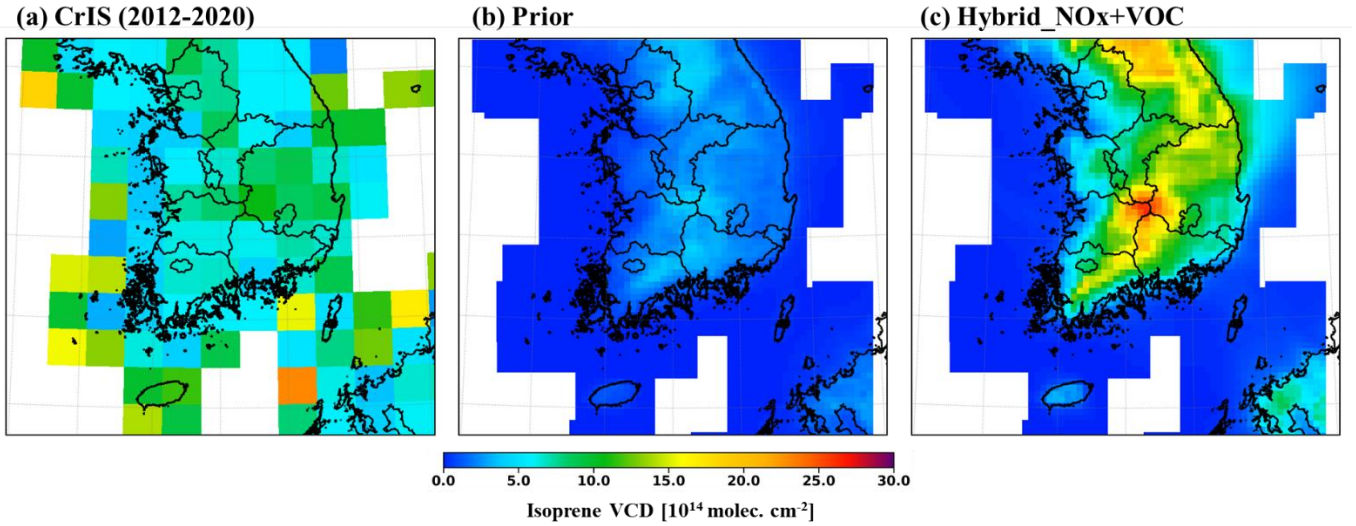

Figure S5: Spatial distributions of isoprene vertical column densities (VCDs) from (a) the May mean CrIS retrievals for 2012–2020, (b) the Prior experiment, and (c) the Hybrid_NOx+VOC experiment. The CMAQ results are averaged over the study period.

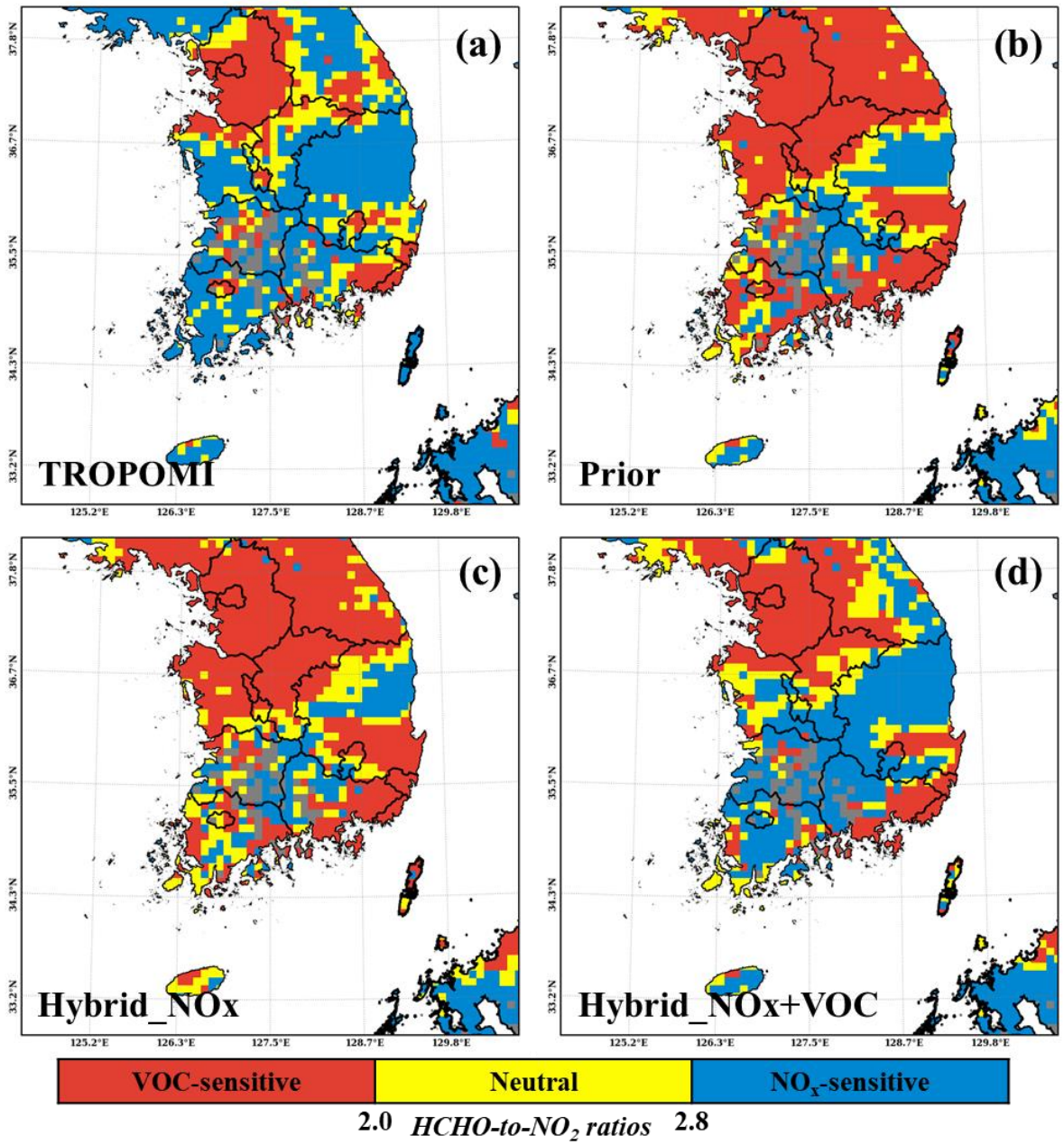

Figure S6: Spatial distributions of O_3 sensitivity regimes for (a) TROPOMI-based HCHO-to-NO_2 ratios, (b) Prior, (c) Hybrid_NOx, and (d) Hybrid_NOx+VOC experiments, averaged over the study period. Red, yellow, and blue indicate VOC-sensitive, neutral, and NO_x-sensitive regimes, respectively. Gray areas denote missing or filtered pixels (e.g., due to cloud interference); for consistency, model results are sampled only at locations and times with valid satellite observations. Oceanic regions are masked to focus on terrestrial emission impacts.

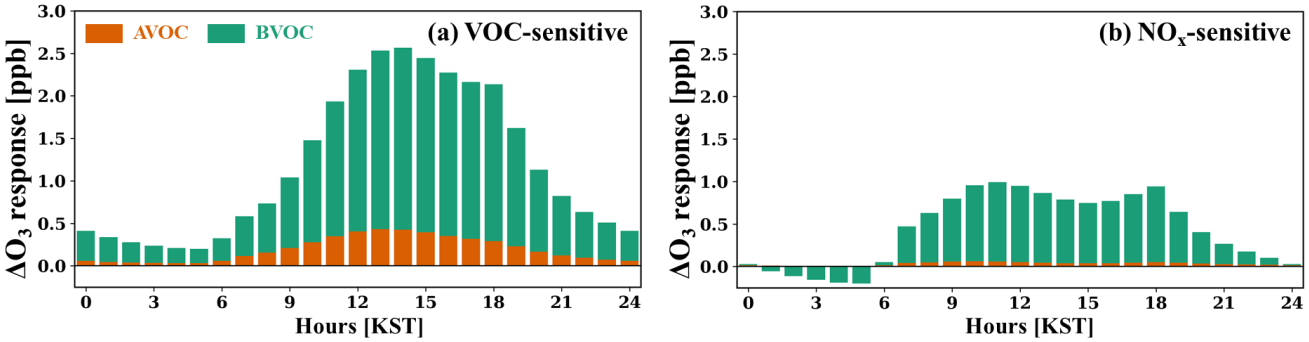

Figure S7: Two-week mean ΔO_3 response (ppb) to anthropogenic VOC (AVOC, orange) and biogenic VOC (BVOC, green) emissions, by local hour, for 1–14 May 2022. For each local hour, responses are spatially averaged over grid cells classified into each regime at that hour; regimes are diagnosed with the HCHO-to-NO_2 ratios from the Hybrid_NOx+VOC experiment. Panels (a) and (b) show, for VOC-sensitive and NO_x-sensitive regimes respectively, the ΔO_3 response at each local hour to emissions released over all hours (i.e., emission-time–integrated response).